JOURNAL OF AGRICULTURAL AND FOOD CHEMISTRY

Article

pubs.acs.org/JAFC

Antioxidants and Physical Integrity of Lipid Bilayers under Oxidative Stress

Ran Liang,[†] Yin Liu,[†] Li-Min Fu,[†] Xi-Cheng Ai,[†] Jian-Ping Zhang,*[,†] and Leif H. Skibsted*[,†,‡]

[†]Department of Chemistry, Renmin University of China, Beijing 100872, China

[‡]Food Chemistry, Department of Food Science, University of Copenhagen, Rolighedsvej 30, DK-1958 Frederiksberg C, Denmark

Supporting Information

ABSTRACT: Giant unilamellar vesicles (GUVs of diameter 5−25 μm) of soy phosphatidylcholine (PC), resistant to intense light exposure (400−440 nm, ∼15 mW·mm^{-2}), underwent budding when containing chlorophyll *a* (Chl*a*) in the lipid bilayer ([PC]:[Chl*a*] = 1500:1). On the basis of image heterogeneity analysis using inverted microscopy, a dimensionless entropy parameter for the budding process was shown to increase linearly during an initial budding process. Lipophilic β-carotene (β-Car, [PC]:[β-Car] = 500:1) reduced the initial budding rate by a factor of 2.4, while the hydrophilic glycoside rutin ([PC]:[rutin] = 500:1) had no effect. Chl*a* photosensitized oxidation of PC to form linoleoyl hydroperoxides, further leading to domains of higher polarity in the vesicles, is suggested to trigger budding. The average dipole moment (μ) of linoleic acid hydroperoxides was calculated using density functional theory (DFT) to have the value of 2.84 D, while unoxidized linoleic acid has μ = 1.86 D. β-Carotene as a lipophilic antioxidant and singlet-oxygen quencher seems to hamper oxidation in the lipid bilayers and delay budding in contrast to rutin located in the aqueous phase. The effect on budding of GUVs as a detrimental process for membranes is suggested for use in assays for evaluation of potential protectors of cellular integrity and functions under oxidative stress.

KEYWORDS: *giant unilamellar vesicles, budding, oxidative stress, bilayer integrity, antioxidant*

INTRODUCTION

Membranes are organizing biological systems, and damages to membranes, unless repaired, are detrimental for cellular functions and cellular integrity.[1] Phospholipids organized in liposomes are often used as model systems for membranal structures, and phospholipase hydrolysis are known to be important for change in surface properties leading to vesiculation and component trafficking through membrane barrier.[2,3] The hydrolytic processes are reversible and enzymatically controlled and may be recognized through formation of rafts in membranal structures.[4] Giant unilamellar vesicles (GUVs), defined as those having diameters of 5−200 μm,[5] are of particular research interest because they have the same scales as the living cells and are observable to optical microscopy. Certain remarkable morphological deformation such as liposome fusion, fission and budding have been observed in GUVs using microscopy related techniques including phase contrast and fluorescence microscopy.[5−11] Because GUV-based experiments are performed at the level of single liposome, heterogeneity in shape and size can be obtained using digital image processing.[10,12,13]

Light-induced morphological deformation processes of fluorescently labeled GUVs are observed under intense irradiation of fluorescence microscope.[14] Chemical reactions of unsaturated fatty acid side chains in lipid molecules, such as polymerization and oxidation initiated via excited states of fluorescence probe or photosensitizer, seem to be the cause of light-induced deformation.[15−17] Oxidative processes also affect membrane properties since the phospholipids and cholesterol as unsaturated lipids easily oxidizable forming lipid hydroperoxides as the primary oxidation product.[15] Oxidative damages of membranes will affect cellular functions and cellular integrity and are often controlled by natural antioxidants integrated in the lipid monolayers or associated with the lipid/water interface.[16,17] Under conditions of increased oxidative stress as may be caused by light exposure as for skin and eye, by catalysis by transition-metal ions during food digestion, or through enzymatic formation of reactive oxygen species (ROS) like hydrogen peroxide and hydroxyl radicals, membrane damage may lead to cellular decay and death.[18]

The increasing interest in redox signaling and regulation of biological systems have led to establishment of a great variety of antioxidant assays in order to evaluate antioxidants for protection of food and for evaluation of health effects of antioxidants.[19−22] However, a direct evaluation of various antioxidants as protectors of vital physical structures seems not available but will depend on indirect methods involving chemical analysis of various oxidation products. We have selected budding as a physical process indicative of damage to GUVs based on soy lecithin (dominant species: dilinoleoyl phosphatidylcholine) as membrane models and applied inverted microscopy and image analysis to monitor the effect of photosensitized oxidation in the presence and absence of potential antioxidants.

Received: July 17, 2012
Revised: September 26, 2012
Accepted: September 27, 2012
Published: September 27, 2012

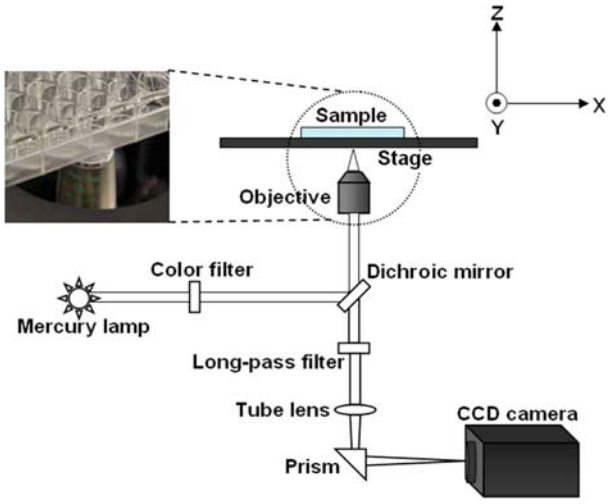

Figure 1. Experimental setup based on inverted microscopy of light exposed GUV and image acquisition by CCD.

MATERIALS AND METHODS

Chemicals and Liposome Preparation. Soybean L-α-phosphatidylcholine (PC, 23%), all-*trans*-β-carotene (β-Car, >95%) and rutin (>95%) were purchased from Sigma Aldrich (St. Louis, MO). Chlorophyll *a* (Chl*a*, >80%) was extracted from fresh spinach leaves and was separated accordingly following ref 23 (see the Supporting Information for details). Sodium dihydrogen phosphate, disodium hydrogen phosphate, methanol and chloroform (all AR) were purchased from Beijing Chemical Works (Beijing, China). Ion-exchanged water was prepared using Milli-Q Academic Water Purification System (Millipore Corp., Billerica, MA).

GUVs were prepared using a reverse phase evaporation method[24] with certain modifications. Briefly, 100 μL of PC predissolved in chloroform (0.1 M) was added to a 100-mL round-bottom flask containing 4.9 mL of chloroform and 750 μL of methanol. β-Car predissolved in chloroform and/or rutin predissolved in methanol (both 10^{-4} M) were added to the flask when needed. Chl*a* (10^{-5} M) predissolved in methanol was added as a photosensitizer to the flask when needed. The final molar concentration ratio of PC and Chl*a* was 1500:1, and that of PC and antioxidants (β-Car and/or rutin) was 500:1. The volume ratio of methanol and chloroform was 1:6.7.

A total of 35 mL of phosphate buffer solution (pH 7.4) was slowly added to the flask along the flask wall. The flask was covered with aluminum foil and kept in a 20 °C water bath and the solvents were slowly removed by rotary evaporation under 0.01 MPa pressure. After evaporation for 2 min, an opalescent suspension of GUV was obtained with a volume of approximately 33 mL.

Monitoring Morphological Changes. GUVs were monitored by means of brightfield and fluorescence microscopy using Eclipse TE-2000U inverted microscope (Nikon Corporation, Tokyo, Japan) with a 40× magnifying objective lens (numerical aperture 0.6, CFI Plan Fluor. ELWD, Nikon). The light sources of brightfield and fluorescence imaging were a tungsten lamp and an ultrahigh pressure mercury lamp, respectively. A 400−440 nm radiation light was obtained by using a dichroic mirror combined with a long-pass filter (see Figure 1), and the power of radiation light was 13 mW for an area of ~0.8 mm^2. The image was detected by a Cascade II 512 semiconductor cooled (−70 °C) CCD with a resolution of 512 × 512 pixels (Photometrics Inc., Tucson, AZ), and the digital images were collected by MetaMorph program package (Molecular Devices, Inc., Sunnyvale, CA).

A total of 200 μL of liposome suspension was added to Costar 24 well cell culturing cluster (Corning Incorporated, Corning, NY), which was placed on the stage of the microscope. Liposome morphology image after radiation was collected for every 5 s, and each GUV suspension preparation was measured 24 times. GUVs without photosensitizer or antioxidant added were used as blank samples, whereas GUVs with photosensitizer added but without antioxidants added were used as control.

Digital Image Analysis. Programs for digital image analysis were coded with MATLAB 7.0 (Mathworks, Inc., Natick, MA), and for each GUV image, an area of 192 × 192 pixels at the center were selected as the region of interest (ROI). Image entropy was selected as a statistical scalar measure of image heterogeneity.[25] Entropy of a grayscale image is defined as:

$$E = -\sum p \log_2 p \quad (1)$$

where p is the histogram (see Figure 2 for example) count over a series of intensity subintervals. The budding process of GUVs was characterized by entropy change compared to the average entropy of negative delaytime data points (before irradiation).

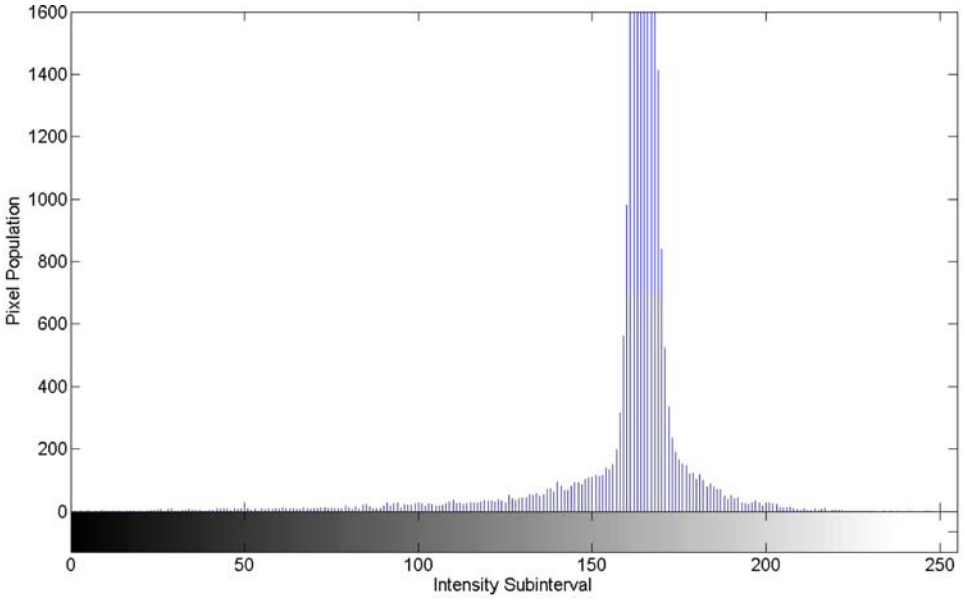

Figure 2. Image histogram example of GUV with Chl*a* and rutin added (Figure 5c) following 25 s of light exposure, forming the basis for calculation of entropy.

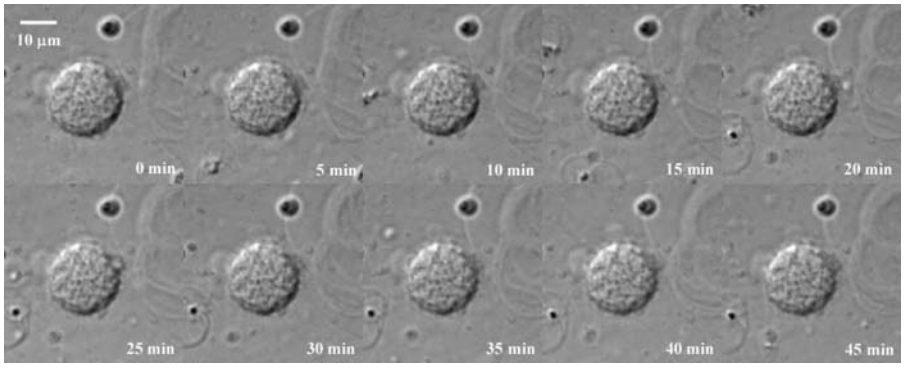

Figure 3. Images of GUV without Chl*a* added exposed to light for up to 45 min.

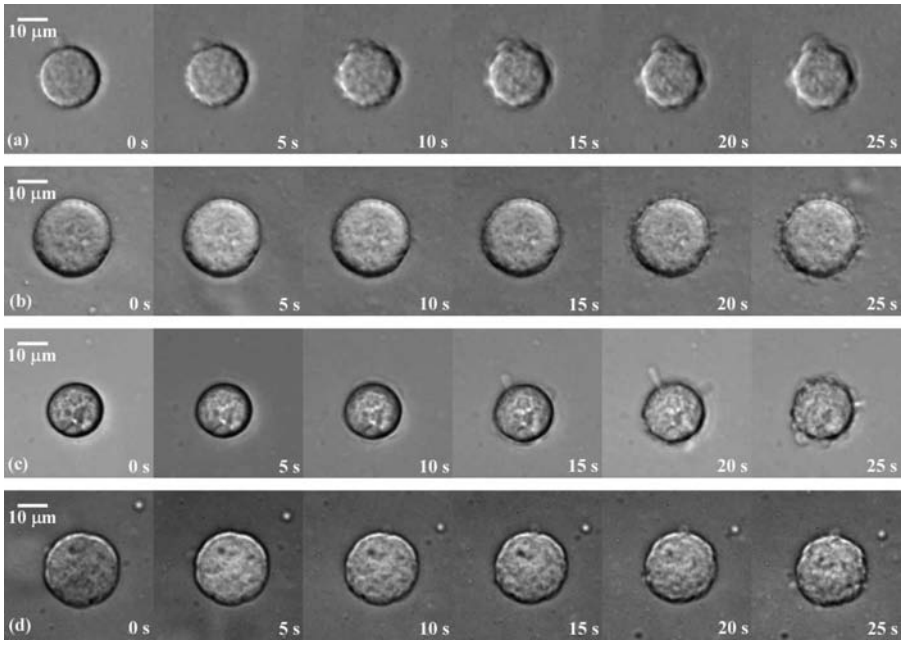

Figure 4. Images of GUV exposed to light for time indicated: (a) with Chl*a*; (b) with Chl*a* and *β*-Car; (c) with Chl*a* and rutin; and (d) with Chl*a*, *β*-Car and rutin.

Quantum Chemical Calculation. Structure optimizations for phospholipids and their hydroperoxides were performed using Gaussian 03W Rev. E01 package.[26] Semiempirical optimization (PM3 method) was carried out to obtain the initial geometries, and then DFT optimization on the basis of B3LYP method and 6-31G** basis set was performed to calculate the dipole moment of each compound.

RESULTS AND DISCUSSION

The GUVs prepared from natural soy PC had a diameter in the 5−25 μm range, calculated on the basis of the pixel size of the CCD detector and the magnifying factor of the objective lens. They did not change in size or shape for up to 60 min when kept in the dark or upon exposure to light in the 400−440 nm region of an intensity of approximately 15 mW·mm^{-2} if no photosensitizer was added, see Figure 1. The integrity of the liposome under these conditions was evident from visual inspection as may be seen from Figure 3. GUVs prepared to contain Chl*a* were, in contrast, sensitive to light exposure as morphological changes were seen already after 5 s and increasing with exposure time as may be seen in Figure 4. On the basis of histograms as the one shown in Figure 2, the texture of the GUV surface was characterized based on image heterogeneity analysis and the dimensionless randomness parameter E (entropy) as defined in eq 1 was calculated. The change in surface entropy with exposure time is shown for GUV with Chl*a* for up to 2 min (Figure 5a). The change in surface entropy increases to a certain value and levels off. To obtain numerical stability, 16 independent experiments formed the basis for calculations for each set of experimental conditions, and the initial rates were determined as the slopes of the $\Delta E-t$ curve during the initial budding processes.

For GUV with the lipophilic *β*-Car added together with Chl*a*, the budding resulted in less morphological changes as may be seen from Figure 4 and as was also evident from the entropy parameter. For ΔE, an almost linear increase is noted from Figure 5b, which levels off at a lower value than for GUV with only Chl*a* added. Rutin, the hydrophilic glycoside of quercetin, had a lower reduction factor of the rate by which ΔE initially increased for GUV with only Chl*a* added (Figure 5c), in agreement with comparable morphological changes of GUV with Chl*a* added alone and for GUV with both Chl*a* and rutin added (Figure 4). The presence of rutin did, however, lower the level of ΔE following longer time exposure of GUV to light (Figure 6). For GUV with Chl*a* added together with both *β*-

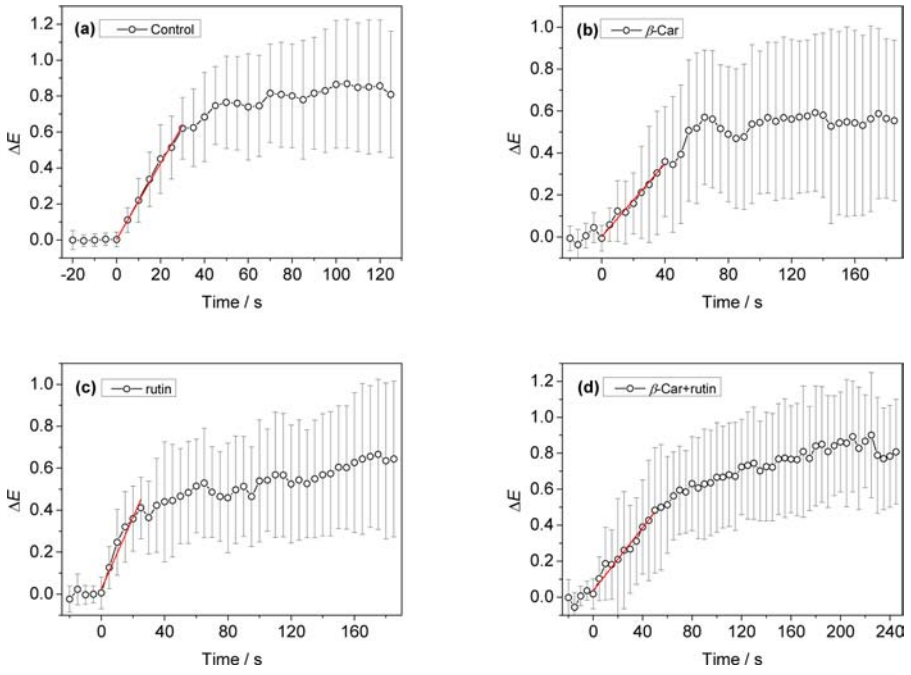

Figure 5. ΔE as an image heterogeneity parameter for GUV with Chl*a* and/or antioxidants exposed to light. Statistics: mean ± SD, n = 16.

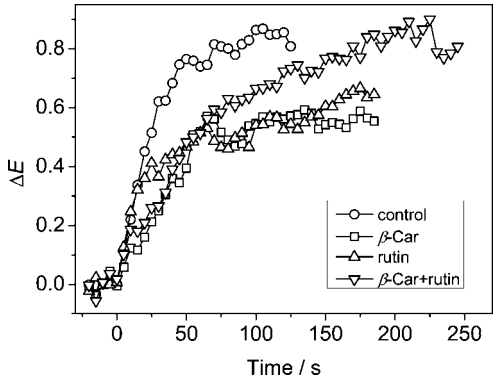

Figure 6. ΔE as an image heterogeneity parameter for GUVs with Chl*a* only (control); with Chl*a* and β-Car; with Chl*a* and rutin; and with Chl*a*, β-Car and rutin.

Table 1. Initial Rates of Increase in ΔE for GUVs Exposed to Light Determined As the Slopes of Initial Stages of ΔE–t Curves (n = 16)

sample	initial rate/s^{-1}
control	$(2.11 \pm 0.04) \times 10^{-2}$
β-Car	$(8.69 \pm 0.54) \times 10^{-3}$
rutin	$(1.71 \pm 0.16) \times 10^{-2}$
β-Car+rutin	$(8.77 \pm 0.57) \times 10^{-3}$

Table 2. DFT-Calculated Dipole Moments for Linoleic Acid and Hydroperoxides on the Basis of B3LYP Method and 6-31G Basis Set**

species	μ/Debye
linoleic acid	1.86
linoleic acid-9-OOH	3.31
linoleic acid-10-OOH	2.25
linoleic acid-12-OOH	3.92
linoleic acid-13-OOH	2.11

Car and rutin, each at the same concentration as in the experiments with one of the potential antioxidant added, the initial rate for increase in ΔE was similar to the rate for ΔE for GUV with Chl*a* and β-Car (Figure 5d). The final level of ΔE was, however, higher for the GUV with both potential antioxidants compared to GUV with only β-Car or rutin (Figure 6). The initial rates for the change in ΔE are in Table 1 collected for the four types of GUV investigated as characterized by their additives.

Budding is related to growth of domains depending on phase separations in vesicles like the GUV studied.[3] For oxidative stress as induced by photosensitized oxidation, such transitions have been proposed to be initiated by oxidative cleavage of unsaturated lipids.[15] For dilinoleoyl PC, as dominated in soy lecithin, formation of hydroperoxides is suggested to initiate changes in surface tension leading to curvature changes and eventually to budding. The dipole moments of linoleic acid hydroperoxides as derived from DFT calculations and shown in Table 2 show a significant change in dipole moment and accordingly polarity as compared to the unoxidized linoleic acid. DFT optimized geometries of unoxidized soy lyso-PC and soy PC and their hydroperoxides are shown in Figure 7. Distortion of unsaturated fatty acid moieties of the lipid molecules is clearly seen in their hydroperoxides. Redistribution of PC in membranes is known to induce shape changes of giant liposomes.[27] The mechanism behind the budding may accordingly be described as following. Chl*a* is absorbing light and forms a triplet state through inner-system crossing from the initially formed singlet excited states. Singlet oxygen is subsequently formed by ground state oxygen ($^3O_2$) quenching the Chl*a* triplet state:[28]

$$\text{Chl}a \xrightarrow{h\nu} {}^1\text{Chl}a^* \quad (2)$$

$${}^1\text{Chl}a^* \xrightarrow{\text{ISC}} {}^3\text{Chl}a \quad (3)$$

$${}^3\text{Chl}a + {}^3O_2 \rightarrow \text{Chl}a + {}^1O_2 \quad (4)$$

dx.doi.org/10.1021/jf3030979 | J. Agric. Food Chem. 2012, 60, 10331–10336

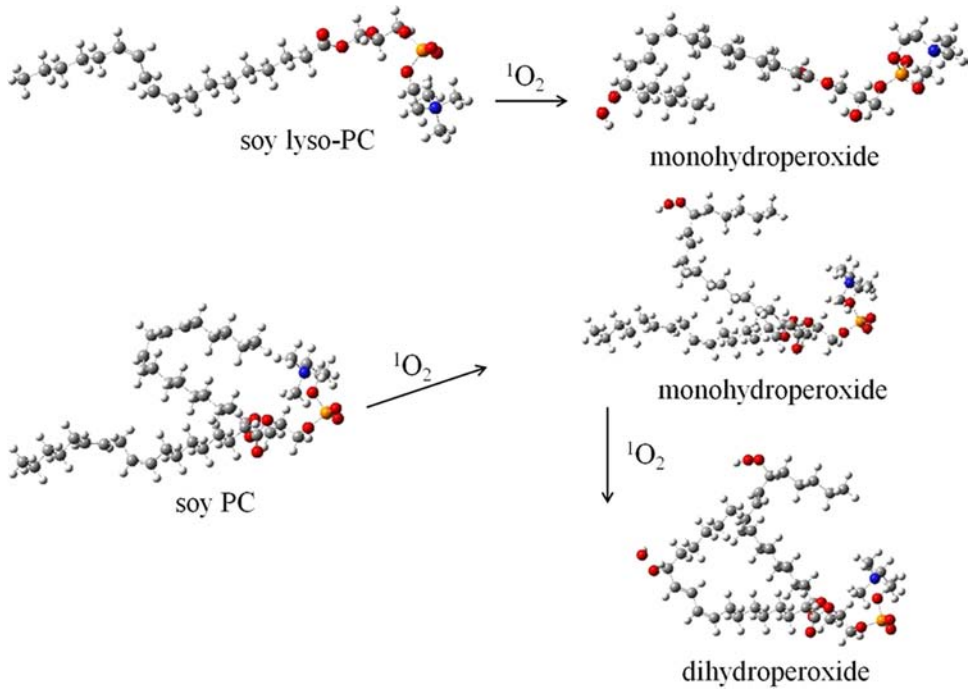

Figure 7. DFT optimized geometries of soy lyso-PC and soy PC and their hydroperoxides on the basis of B3LYP method and 6-31G** basis set.

Singlet oxygen will react with PC to yield hydroperoxides:[29]

$$^1O_2 + PC \rightarrow PC - OOH \text{ or } PC - (OOH)_2 \quad (5)$$

The PC−OOH or PC−$(OOH)_2$ will initiate the morphological changes as seen in Figure 4 and as expressed as ΔE in Figure 5 and 6. The protective effect of β-Car may be assigned to quenching of singlet oxygen [30] in effect competing with the reaction of eq 4 in the lipid layers:

$$^1O_2 + \beta\text{-Car} \rightarrow {}^3O_2 + {}^3\beta\text{-Car}^* \quad (6)$$

$$^3\beta\text{-Car}^* \rightarrow \beta\text{-Car} + \text{heat} \quad (7)$$

Rutin, located in the aqueous phase, will not or only to a small degree, quench the singlet oxygen, providing an explanation for the different effect of the two potential antioxidants on the morphological changes of the GUV. This is also supported by the results of kinetics studies of the singlet oxygen quenching effects of carotenoids and flavonoids. The singlet oxygen quenching rate of rutin in deuterated water (pD 7.4) was determined as 2.4×10^7 M^{-1} s^{-1},[31] whereas β-carotene had the value of 1.0×10^{10} M^{-1} s^{-1}.[32] In the present work, the lipophilic photosensitizer Chl*a* was used, and singlet oxygen was formed primarily in the lipid phase. Therefore, the lipid soluble antioxidant β-carotene had better singlet quenching effect than water-soluble rutin. The rates of initial changes of ΔE further indicate that the efficiency of β-Car in protecting GUV against the morphological changes is independent of the presence of rutin. The different level being reached for ΔE following longer exposure times may depend on other factors such as inner-filter effects or interference from secondary radical processes, including regeneration of β-Car from its radical cation by rutin (anion) at the lipid/water interface.[33]

$$\beta\text{-Car}^{\bullet+} + \text{rutin} \rightarrow \beta\text{-Car} + \text{rutin}^{\bullet} + H^+ \quad (8)$$

Notably, for GUV with Chl*a* incorporated together with both β-Car and rutin, additivity in lowering of the final level of ΔE is not seen, an effect which deserves further studies.

The heterogeneity observed and expressed as the parameter ΔE has been assigned to the budding of GUV. Budding as a morphological change for lipid bilayer is indicative of change in surface tension and surface curvature. We suggest that oxidative stress induced by photosensitized oxidation of bilayer components may be used for evaluation of single compounds or plant extracts as protectives of integrity of organized biological structures and would explore further this approach in future studies.

■ ASSOCIATED CONTENT

Ⓢ Supporting Information

Additional material as noted in text. This material is available free of charge via the Internet at http://pubs.acs.org.

■ AUTHOR INFORMATION

Corresponding Author

*(J.-P.Z.) E-mail, jpzhang@chem.ruc.edu.cn; tel, +86-10-62516604; fax, +86-10-62516444. (L.H.S.) E-mail, ls@life.ku.dk; tel, +45-3533-3221; fax, +45-3533-3344.

Funding

This work has been supported by the Natural Science Foundation of China (20803091) and the Research Funds for the Central Universities, and the Research Funds of Renmin University of China (RUC No. 10XNI007 and 42316355). L.H.S. is grateful for support from the Danish Research Council for Technology and Production as the grant 09-065906/FTP: Redox communication in the digestive tract.

Notes

The authors declare no competing financial interest.

ABBREVIATIONS USED

β-Car, β-carotene; Chl*a*, chlorophyll *a*; DFT, density functional theory; PC, L-α-phosphatidylcholine

REFERENCES

(1) Binder, W. H.; Barragan, V.; Menger, F. M. Domains and rafts in lipid membranes. *Angew. Chem., Int. Ed.* **2003**, *42*, 5802−5827.

(2) Staneva, G.; Angelova, M. I.; Koumanov, K. Phospholipase A_2 promotes raft budding and fission from giant liposomes. *Chem. Phys. Lipids* **2004**, *129*, 53−62.

(3) Julicher, F.; Lipowsky, R. Domain-induced budding of vesicles. *Phys. Rev. Lett.* **1993**, *70*, 2964−2967.

(4) Lipowsky, R. Domains and rafts in membranes—hidden dimensions of selforganization. *J. Biol. Phys.* **2002**, *28*, 195−210.

(5) Menger, F. M.; Gabrielson, K. D. Cytomimetic organic chemistry: Early developments. *Angew. Chem., Int. Ed. Engl.* **1995**, *34*, 2091−2106.

(6) Menger, F. M.; Lee, S. J. Induced morphological changes in synthetic giant vesicles: Growth, fusion, undulation, excretion, wounding and healing. *Langmuir* **1995**, *11*, 3685−3689.

(7) Dobereiner, H. G.; Kas, J.; Noppl, D.; Sprenger, I.; Sackmann, E. Budding and fission of vesicles. *Biophys. J.* **1993**, *65*, 1396−1403.

(8) Bagatolli, L. A. To see or not to see: Lateral organization of biological membranes and fluorescence microscopy. *Biochim. Biophys. Acta* **2006**, *1758*, 1541−1556.

(9) Morales-Penningston, N.; Wu, J.; Farkas, E. R.; Goh, S. L.; Konyakhina, T. M.; Zheng, J. Y.; Webb, W. W.; Feigenson, G. W. GUV preparation and imaging: Minimizing artifacts. *Biochim. Biophys. Acta* **2010**, *1798*, 1324−1332.

(10) Stottrup, B. L.; Nguyen, A. H.; Tuzel, E. Taking another look with fluorescence microscopy: Image processing techniques in Langmuir monolayers for the twenty-first century. *Biochim. Biophys. Acta* **2010**, *1798*, 1289−1300.

(11) Dimova, R.; Aranda, R.; Bezlyepkina, N.; Nikolov, V.; Riske, K. A.; Lipowsky, R. A practical guide to giant vesicles. Probing the membrane nanoregime via optical microscopy. *J. Phys.: Condens. Matter* **2006**, *18*, S1151−S1176.

(12) Haverstick, D. M.; Glaser, M. Visualization of domain formation in the inner and outer leaflets of a phospholipid bilayer. *J. Cell Biol.* **1988**, *106*, 1885−1892.

(13) Haverstick, D. M.; Glaser, M. Visualization of Ca^{2+}-induced phospholipid domains. *Proc. Natl. Acad. Sci. U.S.A.* **1987**, *84*, 4475−4479.

(14) Zhao, J.; Wu, J.; Shao, H.; Kong, F.; Jain, N.; Hunt, G.; Feigenson, G. Phase studies of model biomembranes: macroscopic coexistence of Lα+Lβ, with light-induced coexistence of Lα+Lo phases. *Biochim. Biophys. Acta* **2007**, *1768*, 2777−2786.

(15) Heuvingh, J.; Bonneau, S. Asymmetric oxidation of giant vesicles triggers curvature-associated shape transition and permeabilization. *Biophys. J.* **2009**, *97*, 2904−2912.

(16) Ayuyan, A. G.; Cohen, F. S. Lipid peroxides promote large rafts: Effects of excitation of probes in fluorescence microscopy and electrochemical reactions during vesicle formation. *Biophys. J.* **2006**, *91*, 2172−2183.

(17) Ishii, K.; Hamada, T.; Hatakeyama, M.; Sugimoto, R.; Nagasaki, T.; Takagi, M. Reversible control of *exo*- and *endo*-budding transitions in a photosensitive lipid membrane. *ChemBioChem* **2009**, *10*, 251−256.

(18) Cardoso, D. R.; Libardi, S. H.; Skibsted, L. H. Riboflavin as a photosensitizer. Effects on human health and food quality. *Food Funct.* **2012**, *3*, 487−502.

(19) Wolfe, K. L.; Liu, R. H. Structure activity relationships of flavonoids in the cellular antioxidant activity assay. *J. Agric. Food Chem.* **2008**, *56*, 8404−8411.

(20) Becker, E. M.; Nissen, L. R.; Skibsted, L. H. Antioxidation evaluation protocols: Food quality or health effects. *Eur. Food Res. Technol.* **2004**, *219*, 561−571.

(21) Laguerre, M.; Lopez-Giraldo, L. J.; Lecomte, J.; Barea, B.; Cambon, E.; Tchobo, P. F.; Barouh, N.; Villeneuve, P. Conjugated autoxidizable triene (CAT) assay: a novel spectrophometric method for determination of antioxidant capacity using triacylglycerol as ultraviolet probe. *Anal. Biochem.* **2008**, *380*, 282−290.

(22) Sasaki, K.; Alamed, J.; Weiss, J.; Villeneuve, P.; Lopez-Giraldo, L. J.; Lecomte, J.; Figueroa-Espinoza, M. C.; Decker, E. A. Relationship between the physical properties of chlorogenic acid esters and their ability to inhibit lipid oxidation in oil-in-water emulsions. *Food Chem.* **2010**, *118*, 830−835.

(23) Shioi, Y.; Fukae, R.; Sasa, T. Chlorophyll analysis by high-performance liquid chromatography. *Biochim. Biophys. Acta − Bioenergetics* **1983**, *722*, 72−79.

(24) Moscho, A.; Orwar, O.; Chiu, D. T.; Modi, B. P.; Zare, R. N. Rapid preparation of giant unilamellar vesicles. *Proc. Natl. Acad. Sci. U.S.A.* **1996**, *93*, 11443−11447.

(25) Gonzalez, R. C.; Woods, R. E.; Eddins, S. L. *Digital Image Processing Using MATLAB*; Prentice Hall: Upper Saddle River, NJ, 2003; Chapter 11.

(26) Frisch, M. J.; Trucks, G. W.; Schlegel, H. B.; Scuseria, G. E.; Robb, M. A.; Cheeseman, J. R.; Montgomery, J. A.; Jr., Vreven, T.; Kudin, K. N.; Burant, J. C.; Millam, J. M.; Iyengar, S. S.; Tomasi, J.; Barone, V.; Mennucci, B.; Cossi, M.; Scalmani, G.; Rega, N.; Petersson, G. A.; Nakatsuji, H.; Hada, M.; Ehara, M.; Toyota, K.; Fukuda, R.; Hasegawa, J.; Ishida, M.; Nakajima, T.; Honda, Y.; Kitao, O.; Nakai, H.; Klene, M.; Li, X.; Knox, J. E.; Hratchian, H. P.; Cross, J. B.; Bakken, V.; Adamo, C.; Jaramillo, J.; Gomperts, R.; Stratmann, R. E.; Yazyev, O.; Austin, A. J.; Cammi, R.; Pomelli, C.; Ochterski, J. W.; Ayala, P. Y.; Morokuma, K.; Voth, G. A.; Salvador, P.; Dannenberg, J. J.; Zakrzewski, V. G.; Dapprich, S.; Daniels, A. D.; Strain, M. C.; Farkas, O.; Malick, D. K.; Rabuck, A. D.; Raghavachari, K.; Foresman, J. B.; Ortiz, J. V.; Cui, Q.; Baboul, A. G.; Clifford, S.; Cioslowski, J.; Stefanov, B. B.; Liu, G.; Liashenko, A.; Piskorz, P.; Komaromi, I.; Martin, R. L.; Fox, D. J.; Keith, T.; Al-Laham, M. A.; Peng, C. Y.; Nanayakkara, A.; Challacombe, M.; Gill, P. M. W.; Johnson, B.; Chen, W.; Wong, M. W.; Gonzalez, C.; Pople, J. A. *Gaussian 03W*, Revision E.01; Gaussian, Inc.: Pittsburgh, PA, 2003.

(27) Farge, E.; Devaux, P. F. Shape changes of giant liposomes induced by an asymmetric transmembrane distribution of phospholipids. *Biophys. J.* **1992**, *61*, 347−357.

(28) Ramel, F.; Birtic, S.; Cuine, S.; Triantaphylides, C.; Ravanat, J. L.; Havaux, M. Chemical quenching of singlet oxygen by carotenoids in plants. *Plant Physiol.* **2012**, *158*, 1267−1278.

(29) Choe, E.; Min, D. B. Chemistry and reactions of reactive oxygen species in foods. *Crit. Rev. Food Sci. Nutr.* **2006**, *46*, 1−22.

(30) Sun, Y.-J.; Pang, J.; Ye, X.-Q.; Lii, Y.; Li, J. Quantitative structure-activity relationship study on the antioxidant activity of carotenoids. *Chin. J. Struct. Chem.* **2009**, *28*, 163−170.

(31) Morales, J.; Guntuer, G.; Zanocco, A. L.; Lemp, E. Singlet oxygen reactions with flavonoids. A theoretical-expemential study. *PLoS ONE* **2012**, *7*, e40548.

(32) Ouchi, A.; Aizawa, K.; Iwasaki, Y.; Inakuma, T.; Terao, J.; Nagaoka, S.; Mukai, K. Kinetic study of the quenching reaction of singlet oxygen by carotenoids and food extracts in solution. Development of a singlet oxygen absorption capacity (SOAC) assay method. *J. Agric. Food Chem.* **2010**, *58*, 9967−9978.

(33) Liang, R.; Chen, C.-H.; Han, R.-M.; Zhang, J.-P.; Skibsted, L. H. Thermodynamic versus Kinetic Control of Antioxidant Synergism between β-carotene and (iso)flavonoids and their glycosides in liposomes. *J. Agric. Food Chem.* **2010**, *58*, 9221−9227.